5-2011

Analysis of Prominent Decay Modes for the Higgs Boson at the LHC

Matthew Parenti
University at Albany, State University of New York

Analysis of prominent decay modes for the Higgs boson at the LHC

Mathew Parenti

11

I. Introduction

Constructed to test the boundaries of particle physics, the Large Hadron Collider (LHC) will be responsible for expanding the knowledge of the Standard Model and will be at the forefront of particle physics research for the next several years. Located over 150 meters under the city of Geneva in Switzerland with a circumference of 27 kilometers, the LHC is the largest particle accelerator in the world. Although the collider will be answering questions for a broad range of topics in particle physics, the most significant findings are expected to be surrounding the Higgs boson, a theoretical Standard Model particle. If evidence of the Higgs boson is found, it will help to prove the existence of the Higgs mechanism, which proposes that all mass is derived from a particles interaction with a non-zero field that pervades all space, even in a vacuum. By studying different Higgs decays for a range of masses, spanning between roughly 80 GeV to more than 1 TeV, scientists at the LHC are hoping to prove the existence of this field. For lower masses, decays into two photons show promise for a Higgs discovery. Higgs decay into ZZ* particles are expected to yield results for intermediate masses between the mass of one and two Z bosons. Beyond a two Z mass, decays into two Z bosons will dominate and are expected to have the best chance for finding the Higgs since much of the background is reducible. By analyzing these prominent decay modes, researchers are optimistic that the riddle of how mass is derived will be solved in the upcoming years.

II. The Large Hadron Collider

The LHC was designed to collide bunches of both protons and heavy ions. At peak capacity, the LHC is capable of colliding 10^{11} protons in 2800 bunches at a rate of 40 million collisions per second. This will result in 14 TeV of energy and a luminosity of 10^{34} cm^{-2} s^{-1}. Lead nuclei are expected to collide with a luminosity of 10^{27} cm^{-2} s^{-1} and an energy of 5.5 TeV for each pair of nucleons when used (CERN.*The* 1). Recently, the LHC has been operating at only half of its designed capacity, colliding beams with energies of 3.5 TeV, with a total of 7 TeV per collision due to mechanical difficulties. Since the collider is not operating at its full capacity, a luminosity of only $4.67x10^{32}cm^{-2}s^{-1}$ has been attained so far. As a precaution against the erosion caused by high counting rates, experimenters designed all materials with the capacity to handle five times above expected radiation levels. The majority of these particles will be tracked by the different calorimeters installed around the central beam axis. Some particles, muons for example, pass through the calorimeters undisturbed. Therefore, it is the responsibility of the muon spectrometer to gather the appropriate data. In order to accomplish this, a strong magnetic field is provided by three air-core toroids, which surround the different calorimeters. The toroids produce a magnetic field of 2 Tesla that is used to bend muons into the detectors, which then determine the path and eventual momentum of the particles (CERN.*The* 5). As particle bunches collide, untold amounts of debris will fly out in the form of photons, electrons, hadrons, baryons, and muons. In the initial tracking chambers nearest the interaction point, neutrons and photons will pass through undetected, while electrons and positrons, hadrons, and muons are detected but still pass through undisturbed. The next level contains the electromagnetic calorimeters, which still detect muons and hadrons, but allow them to pass through uninhibited. Neutrons pass through undetected as well, while electrons and photons are stopped and have their momenta recorded. The hadron calorimeters follow the electromagnetic calorimeters, and are responsible for recording the momenta of differing hadrons, such as protons, pions, and neutrons. The outermost layers are composed of muon chambers that surround the barrel and endcaps, and collect data in both the bending and non-bending directions.

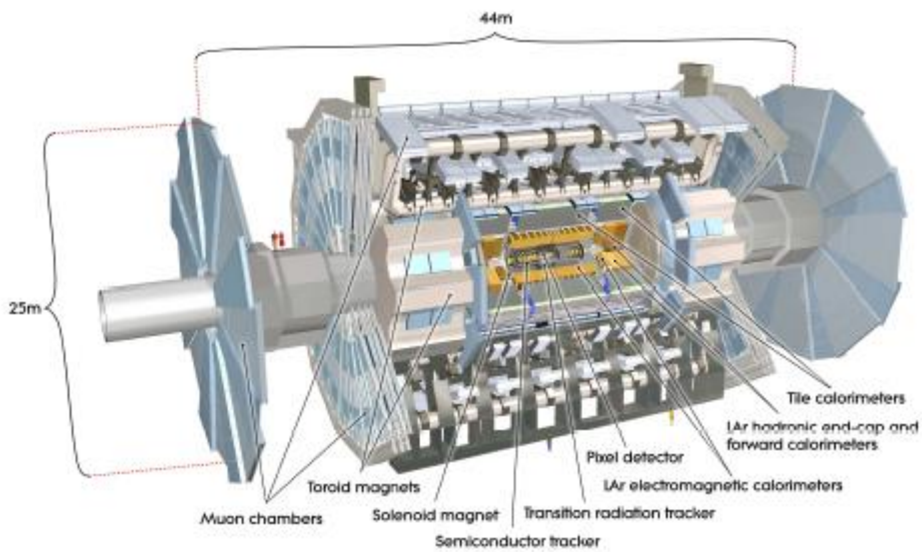

A dissected view of the ATLAS detector (CERN.The 4)

III. Inner Detector

In the areas nearest the interaction point, with a pseudorapidity angle $\eta < 2.5$, the inner detector is positioned as close as physically possible to the interaction point in order to best detect all particles, especially those with the shortest lifetimes. However, due to the close proximity to the center of the detector, the machines must be equipped to handle the intense radiation caused by the 40 million collisions per second. The large number of collisions therefore causes a drop in detector efficiency for measuring low momentum particles with energies lower than .5 GeV (CERN.*The* 298)

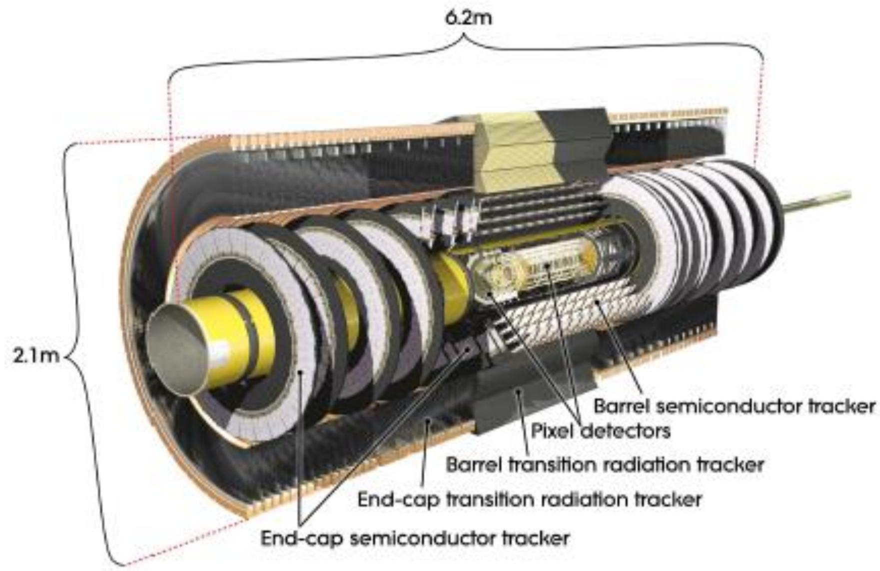

A dissected view of the ATLAS inner detector (CERN.The 6)

Pixel Detectors

In order to handle the extreme rates closest to the collision point, Pixel Detectors must have the absolute highest resolution and be extremely efficient in order to determine the path of the each particle. More than 82 million pixels are used to pinpoint any position with accuracies greater than 14µm. The Pixel Detectors themselves consist of three barrels with three disks on both sides of the barrels surrounding the collision point. The sensors are constructed to be as thin as possible, roughly 250 µm, in order to maximize the flow of particles through the detector (CERN.*The* 57).

Semi- Conductor Tracker (SCT)

Succeeding the Pixel Detector is the Semi-Conductor Tracker. These must also be constructed thinly, having a thickness of roughly 285 µm (CERN.*The* 58). Utilizing eight silicon microstrip sensors, the SCT's have an accuracy of roughly 20 µm and give eight different measurements for every track (CERN.*ATLAS* 12). Following the Pixel and SCT's in the Inner Detector are the Transition Radiation Trackers.

Transition Radiation Trackers (TRT)

This portion of the inner detector relies upon thousands of gas filled 4mm diameter straw shaped tubes to calculate the position of a passing particle. In the barrel region, the tubes are approximately 144 centimeters long, while only being 37 centimeters in the end-caps ("Transition"). As the gas is ionized from the traveling charged particles, electrical signals are produced and allow the particle's distance to be determined from the gold plated tungsten wires in the center of the straws. Electrons that pass through this section can be identified easily because they interact with certain materials in the TRT and produce X-Rays as a byproduct (CERN.*ATLAS*). This greatly aids in particle separation.

IV. Calorimeters

Surrounding the inner detectors are the different calorimeter systems used to determine the energies of the incoming particles. Two types of calorimeters, Electromagnetic and Hadronic, encompass the barrel, end caps, and forward region and are located in three different cryostats used to maintain the temperature below -185˚ Celsius. Otherwise, the liquid argon used to measure the energies of the particles will turn into its gaseous form reducing the effectiveness of the calorimeter system (Brookhaven).

Electromagnetic Calorimeter

In the Electromagnetic Calorimeters, the first of the two, the liquid argon lies between lead absorber plates and electrodes and is arranged in a circular, accordion fashion. This helps to quicken the signal response time over the entire apparatus and allows several layers to work at one time. When electrons or protons penetrate the argon, the electrodes record the ions produced and transfer their signal to nearby electronic devices which can store and analyze the data. Particles that pass through the Electromagnetic Calorimeter then pass through the Hadronic Calorimeter (CERN.*ATLAS*).

Hadronic Calorimeter

Instead of lead, like in the Electromagnetic Calorimeter, the Hadronic Calorimeter uses steel as the absorber and plastic scintillator tiles between the steel. As ionized particles permeate the tiles, their energies cause light to be emitted. The light is then transferred by fibers to photon detectors, which transform the light into electrical signals that can be stored and evaluated later (CERN.*ATLAS*).

V. Muon Spectrometer

The muon spectrometer is responsible for recording the momentum of muons as they pass through the magnet system that succeeds the first solenoid magnet. Since muons can pass through the inner detector undisturbed, it is possible for the different portions of the spectrometer to record the various momenta as they are bent by the magnet (Brookhaven. “ATLAS Muon…”).

Monitored Drift Tubes (MDT)

The chambers that perform the majority of the muon detection are known as the Monitored Drift Tubes (MDT’s), which surround the Inner Detector and Calorimeter systems. In total, there are 1150 different tube chambers in the MDT system. The MDT’s operate over the pseudorapidity angle $2.7 > |\eta|$, and are responsible for recording the momentum of muons in the bending direction of the magnet. Each chamber is composed of six layers of tubes stacked upon one another, with each tube having a diameter of 30 mm (Harvard). In order to increase measurement accuracy of the tubes, eight layers are used in the inner detector. On average, however, each tube has a resolution of roughly 80μm and will point in the ϕ direction. The MDT's use a gas mixture consisting of 93 percent Argon and 7 percent Carbon Dioxide, with less than 1000 ppm of water, at a pressure of three Bar. Since this mixture is not known to leave residue or buildup on any of the wires, it was chosen as the preferred operating gas. Despite this advantage, the gas causes resolution discrepancies as the counting rate increases, and it also has a drift time higher than that of most linear gases. On the other hand, constructing the MDT's as a combination of tubes offers several advantages. First, the large number of tubes per chamber allows the detectors to function normally even if a tube fails. This also simplifies the replacement of malfunctioning hardware. Additionally, the accuracy does not heavily rely on a particle's incident angle. Instead it relies on the tangent of the track with respect to the radius of the wire (CERN. *The* 170). However, this setup sometimes causes additional track hits to occur.

Cathode Strip Chambers (CSC)

Unfortunately, the MDT's are only capable of accurately handling angles up to a pseudorapidity of 2 in the first end cap layer, which sees particle rates that surpass the limit for the MDT to remain accurate. Instead, between $2 < |\eta| < 2.7$, they are replaced by Cathode Strip Chambers (CSC's), which are capable of handling counting rates of up to 1000 Hz/cm^2 and also have superior time resolution (CERN. *The* 178). These are eight small and large chambers surrounding the end caps, seven meters from the interaction point, consisting of five panels of cathode strips with anode wires arranged between each strip (CERN. *The* 183). A combination of argon and carbon dioxide surrounds the anode wires, which then becomes ionized after particles pass through the chamber. The electric charges produced allow the CSC to record the position of a particle with a resolution of 60μm (CERN. *The* 179). Since the position is measured in this way, it allows external stimuli, for instance temperature change, pressure change, and gas gain, to have no effect on the chamber readings, increasing the accuracy of the CSC.

Thin Gap Chambers (TGC)

Due to the sheer volume of data available from the millions of collisions occurring every second, it would be impossible to look at every collision and find any meaningful information. Thus, trigger systems were designed to filter out the majority of the unimportant data, leaving a manageable amount of information that can be collected and analyzed. Thin Gap Chambers (TGC's) are one of the initial trigger systems used due to their efficiency and great time resolution. A TGC functioning normally will have an efficiency of greater than 99 percent, and most trigger chambers in general will have time resolutions between 1.5 and 4 nanoseconds (CERN. *The* 199). In addition to being a trigger system, the TGC's can measure particle coordinates in both the bending and non-bending direction. The measurement in the non-bending direction is used in conjunction with the MDT readings to provide a second, azimuthal direction to the coordinates (CERN. *ATLAS*). In order to get these measurements, the TGC's were constructed as discs that encircle the end cap in between $1.05 > |\eta| > 1.92$, and also in the forward region between $1.92 > |\eta| > 2.4$. In the end cap region there are three TGC systems in place, while the inner tracking region has two TGC layers and the middle tracking layer has seven TGC layers. Both the inner and middle regions allow azimuthal measurements of incoming particles, but it is only the middle seven layers that are used as the trigger system (CERN. *The* 200). Using information gathered from the different detectors, the trigger system detects muons that get energized and released at every bunch crossing.

Resistive Plate Chambers (RPC)

Comparable to the TRT's, the trigger mechanism in the barrel is performed by several surrounding layers of Resistive Plate Chambers (RPC's). These chambers are paired with the MDT's in the region surrounding the barrel. Two layers of RPC's surround the middle MDT's, and a third is in the area around the outer MDT. These three RPC's provide experimenters with exceptional space and time resolution, and can handle moderate counting rates. The RPC's are also responsible for providing the second, azimuthal coordinate for the MDT's (CERN. *ATLAS*). In addition, RPC's use the ionized gases in the chambers to measure the curvature of the muon tracks to determine if the particle has surpassed a certain momentum. If the muon has a desirable momentum value, its data is kept and transmitted to the next level of triggers. Otherwise, the information is discarded. The RPC's are composed of two parallel resistive plates that generate an electric field in the two millimeters of space between the plates, which are roughly thirty to forty millimeters in width. As muons pass through, the electric field generates signals which are then sent to be read out elsewhere. RPC's are capable of operating in two separate modes, avalanche mode and streamer mode. However, avalanche mode is the preferred mode for ATLAS due to the larger rates and time independence associated with this mode selection (CERN. *The* 195). This helps to nullify the elevated background rates experienced at the detector.

VI. Higgs Mechanism

In the Higgs mechanism, the Lagrangian of the minimum energies of two fields is taken, assuring that it is invariant with respect to local gauge transformations. In order for this to be accomplished, a new gauge particle must be added to the Lagrangian. This results in a Goldstone boson being absorbed into a gauge particle, which then acquires a mass from the absorbed particle. The absorption also increases the polarization of the system from two to three states. As a result, the absorbed Goldstone boson acts as the third, longitudinal polarization state for the Goldstone boson. Subsequently, a new massive particle of spin 0, now called the Higgs boson, and gauge field are created from this process (Coughlan 107). In the Standard Model, the masses of the gauge bosons, $W^{\pm}$ and Z^0, used in weak force interactions are derived from this mechanism. Therefore, the discovery of the Higgs boson can demonstrate that gauge theories can be applied to all fundamental forces, showing that each can be ascertained by mechanisms such as this.

Spontaneous Symmetry Breaking

The Higgs mechanism elaborates that there exists a non-zero scalar field that pervades all space, including that of a vacuum. Normally, the lowest energy state of a field occurs when the field has a value of zero; however, in the case of the Higgs mechanism, the lowest energy state is obtained through a non-zero field value. The expectation value produced through the process of spontaneous symmetry breaking results in the creation of boson and fermion mass. The idea of spontaneous symmetry breaking is often likened to that of a person squeezing a small strip of plastic. When the top and bottom are squeezed together and enough pressure is applied, the strip will bend in an outward direction. Consequently, the new "lowest energy" equilibrium state of the strip is in this curved position, which can be in any number of directions. Therefore, the positional "symmetry" of the strip is broken. When this even occurs with no external stimuli, as in the case of the Higgs mechanism, it is referred to as spontaneous (Griffiths 375). When this is translated into concepts such as group theory, an initial broken symmetry group gets reduced to a subgroup of that symmetry (Brading). In the case of the plastic strip after symmetry is broken, the energy is at a minimum along the circle given by $R^2 = \phi_1^2 + \phi_2^2$, instead of 0 (Coughlan 105). Taking the Lagrangian of a particle using this reference will then show how the components of the particle in this system will interact when the energy is at a minimum. By shifting the system to be centered around a point R on the radius of the previously defined circle; this process can be better facilitated.

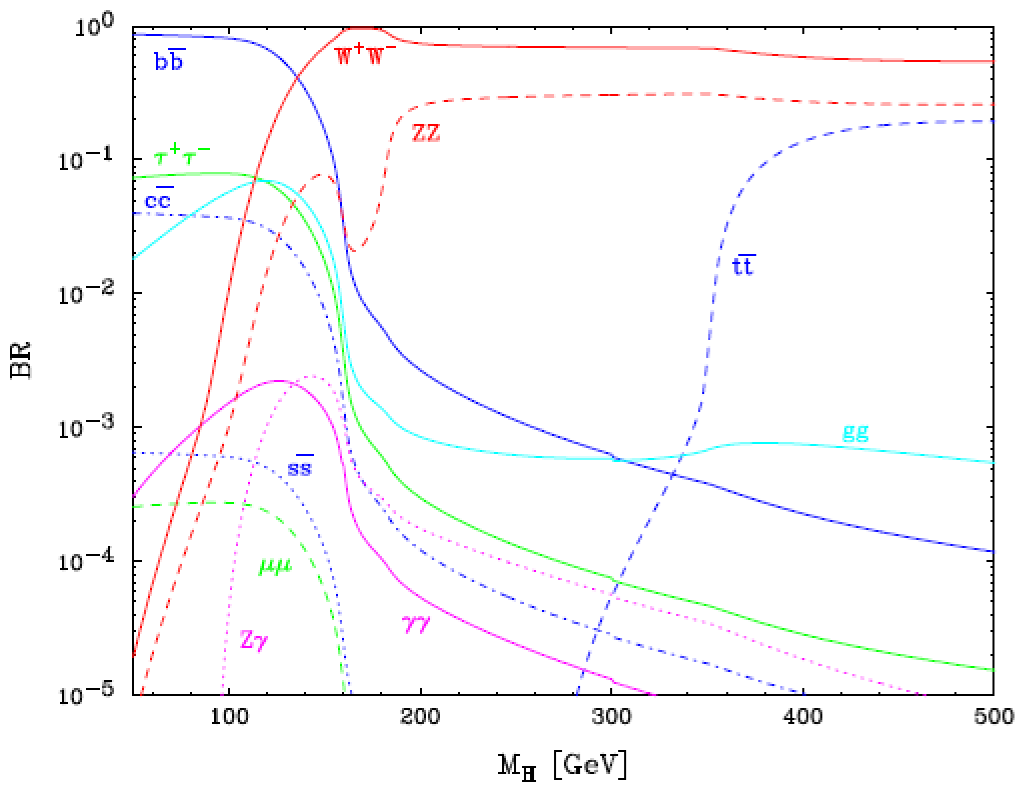

Graph illustrates several Higgs branching ratios plotted as a function of mass (A. Djouadi)

VII. Prominent decay modes

Higgs decay into two photons $H \rightarrow \gamma\gamma$

The LHC will provide an abundance of Higgs decay channels; however, depending on the presence of background rates, some decays will exhibit superior results when compared to others at certain masses. While the top quark Higgs production was initially regarded as a near guaranteed way to find a lower mass Higgs, further input revealed that background rates were far too high to yield any tangible results. The ttbb and ttjj backgrounds were found to greatly reduce the ability to find an accurate Higgs mass peak within the data. Even though this avenue is not expected to produce reliable Higgs data, it still can provide evidence for rare decays into photons. (Rainwater 23). Instead, Higgs decays into photons, $H \rightarrow \gamma\gamma$, for example, are considered impractical except for lower masses from 90 to around 140 GeV (Dorigo). By referring to the preceding graph, one can see the branching ratio of the Higgs decay into two photons peaks at a value near 10^{-3}, between 120 and 140 GeV, and then suddenly plummets. In translation this means that for lower masses Higgs decays into two photons will occur for only .1 percent of the cases. Although the smaller branching ratios of this decay mode lead to a more dynamic and difficult to find final state, it allows for a better readout due to less background. This is attributed to the relationship between collision energy and background particle rates; as the interaction energy increases, so do the cross section and background rates. Therefore, a positive identification for this process is more significant when compared to a high cross section hit with a large background, for example $H \rightarrow b\bar{b}$. Even though the bottom quark decay dominates this mass range, the tendency for the quarks to form jets leads to a nearly unmanageable amount of jet production (Egede). This, when coupled with the photon's easily identifiable track pattern and ability to discern jet fakes, make this decay mode a reliable means for discovering light Higgs particles. The most likely contributors for two photon Higgs decay will consist of either two different $W^{\pm}$ Feynman loops or the interaction of top quarks, illustrated below.

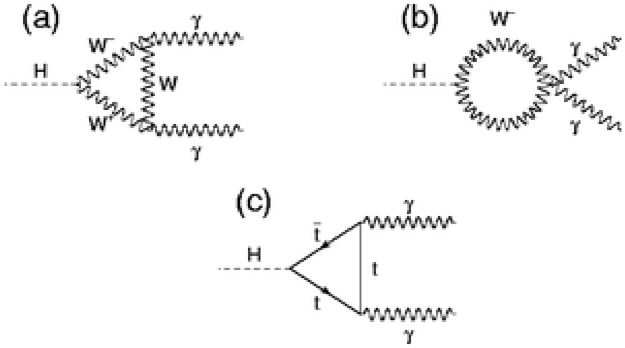

Top three Feynman diagrams for higgs decay into two photons (Dorigo).

Background for γγ

Even though two photon decays at this energy level produces very clean signatures in the calorimeter, background production can still hinder progress since a Higgs decay into two photons will not be the only process that will produce photons. A significant amount of excess photons are produced through the decays of neutral hadrons. For example, π° primarily decays into two photons, and it is also possible for η to perform this process. π° is also responsible for producing jet fakes, where the majority of the pions energy is recorded by the calorimeter as it decays, causing the transferred energy to appear as a photon (Egede). Background can also be created through the Bremsstrahlung process, where an electron can emit a photon as it passes another charged particle such as an atomic nucleus. Because of this process, electrons can lose a majority of their momentum before even hitting the calorimeters. This can reduce efficiency because it is possible for the electrons to have insufficient energy to record a valid measurement in the calorimeter (CERN.*The* 106).

Decay from *H → ZZ(*) → 4l*

However, the branching ratio for two photon decay begins to drop significantly at around 140 GeV, making the *H → ZZ** → 4l production channel the most prominent channel for a Higgs decay to occur for intermediate masses ranging between one Z and two Z bosons. For larger masses up to and even surpassing 600 GeV, the most likely decays will involve decomposition of the Higgs into two Z bosons which subsequently decay into four leptons. Jets or neutrinos can also be produced for the most massive Higgs particles (CERN.*The 2*). However, for the decay channel *H → ZZ* → 4l, generally four muons or electrons are the produced leptons. If the leptons are muons, they will travel through the majority of the detector uninhibited, allowing them to be identified without much difficulty once they reach the muon spectrometer section of the detector. If electrons are produced, they will generally leave clean tracks for higher masses surpassing 500 GeV (Finding).

***Background for H → ZZ(*)* → 4l:**

This mode shows much promise due to the minimal background associated with the decay, as well as its great resolution that surpasses 1 GeV. A majority of the background caused by alternate decays can be reduced to extremely low levels for both ZZ* and ZZ decays . Techniques such as isolating the leptons and restricting the masses of the lepton pairs reduce the background considerably (Egede). There are, unfortunately, downsides to these background reducing constraints. The more the background is restricted, the less efficient the trigger system becomes. Trigger efficiency also suffers as the processing speed increases (CERN.*The* 363). Since they evaluate information more quickly, there is a higher probability that important data will be overlooked and discarded. Thus, researchers need to be cautious when attempting to reduce background rates. For both ZZ and ZZ* decays, however, the primary contributor to the background rates will be normal, isolated ZZ particles that decay into four leptons.

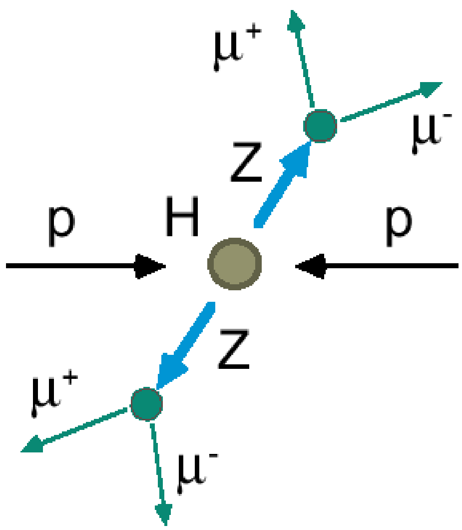

Feynman diagram depicting a Higgs decaying into two Z particles and four muons (Dam)

VIII. Data Analysis

For all of the decay channels, a total of 10 fb^{-1} should sufficient to prove or disprove the Higgs with an uncertainty of 5σ for a majority of the decay channels (Dam). However, at current luminosities, only 1 fb^{-1} of data is expected to be collected by the end of 2011. If this goal is attained, it is believed that this data will narrow the possible Higgs masses significantly by eliminating the mass range between 120 and 530 GeV. Therefore, the decay of a light Higgs into two protons can be potentially disproved by the end of the year due to the mass constraints for that mode unless a positive identification is made. This, along with data collected by the Tevatron collider which eliminated the masses between 158 and 173 GeV, is expected to remove roughly 80 percent of the possible Higgs masses, giving researchers an improved chance of discovery by allowing them to focus on a smaller mass range (Grim). Since the luminosities are also expected to gradually increase as time goes on, experimenters are expecting to reach at least

5 fb^{-1} the following year in 2012. Once this amount of data is obtained, the Higgs mechanism will either be disproved or at least some detection of the Higgs boson will occur on a 95 percent confidence interval (Grim). That is, if the experiment were repeated a large amount of times, 95 percent of the cases will yield results inside the interval. By studying the graph below, which was taken from CMS projections, one can see the effect the amount of data has on the significance level for varying Higgs masses. As more data is taken, the significance of observation increases greatly for certain masses, especially for masses between 150 and 200 GeV, which is in the range for the $H \rightarrow ZZ^* \rightarrow 4l$ decay channel. A positive identification here with the highest peak reaching almost 10 σ at a mass of 160 GeV at ideal luminosity would make any error incredibly unlikely. For example, a value of 1.96 σ corresponds to a confidence interval of 95%, while a value of 5 σ corresponds to a confidence interval of 99.9999994%. As a result, intervals with a significance of 5 σ or larger are extremely reliable sources of data and can prove or disprove the Higgs mechanism once enough data is collected to reach this level.

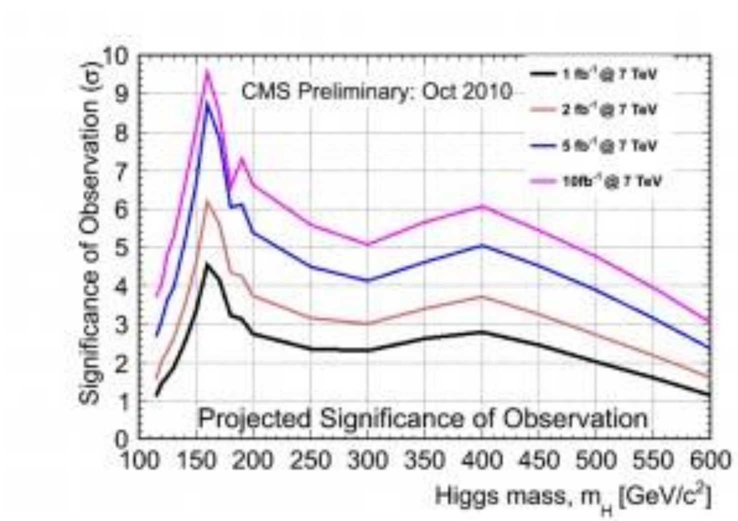

Projected significance levels for a range of Higgs masses at different luminosities at CMS (Grim)

IX. Analysis and Conclusions

In the upcoming years as more data is collected and processed, it will become increasingly clear whether or not there is evidence of a Higgs boson, or if the theory needs to be rewritten. As discussed in the previous section, 1 fb^{-1} will be enough to eliminate an estimated 80 percent of possible Higgs masses. As time goes on, this percentage will only increase. Due to reduced background rates, it is still for a lower mass Higgs to be produced by two photon decay, despite the rarity of the decay. For masses surpassing the 140 GeV limit it is more likely for decays into ZZ* to occur. Masses surpassing 2Z up to roughly 600 GeV will be dominated by the decay of two Z bosons into four leptons. This mode is expected to have the best chance of success because of the large amount of reducible background and also its broad mass coverage. Although the LHC will not reach its maximum power output of 14 TeV until 2014, the amount of data gathered by the end of the upcoming years should be sufficient in narrowing down possible masses for the Higgs in the next few years. In all likelihood the mass will probably fall within the range of the ZZ decay, but judging by how much modern physics has changed over the past century anything can happen.

References

A. Djouadi, J. Kalinowski and M. Spira, Comput. Phys. Commun. 108, 56 (1998).

Bernardi, G., M. Carena, and T. Junk. "HIGGS BOSONS: THEORY AND SEARCHES." Thesis. University of Paris, 2007. 16 July 2008. Web. Mar. 2011. <http://pdg.lbl.gov/2008/reviews/higgs_s055.pdf>.

Brading, Katherine and Castellani, Elena, "Symmetry and Symmetry Breaking", *The Stanford Encyclopedia of Philosophy (Fall 2008 Edition)*, Edward N. Zalta (ed.), URL = <http://plato.stanford.edu/archives/fall2008/entries/symmetry-breaking/>.

Brookhaven. "ATLAS Calorimeter." Brookhaven & the Large Hadron Collider. Brookhaven, 2011. Web. Apr.-May 2011. <http://www.bnl.gov/atlas/lar.asp>.

Brookhaven. "ATLAS Muon Spectrometer." Brookhaven & the Large Hadron Collider. Brookhaven, 2011. Web. Apr.-May 2011. <http://www.bnl.gov/atlas/muon.asp>.

CERN. *ATLAS: The Technical Challenges*. CERN. *Atlas.ch*. CERN, May 2007. Web. Apr.-May 2011. <http://atlas.ch/atlas_brochures_pdf/tech_brochure.pdf>.

CERN. *The ATLAS Experiment at the CERN Large Hadron Collider*. Tech. Institute of Physics & SISSA, 2008. Print.

Coughlan, Guy D., James E. Dodd, and Ben M. Gripaios. "Spontaneous Symmetry Breaking." The Ideas of Particle Physics: an Introduction for Scientists. Cambridge [u.a.: Cambridge Univ., 2006. 105-07. Print.

Dam,Mogens. *Http://atlas.web.cern.ch/Atlas/GROUPS/PHYSICS/Conferences/2003/aspen-03_dam.ppt*. Copenhagen: Niels Bohr Institute, Jan. 2003. Ppt.

Dorigo, Tomasso. "Higgs Decays to Photon Pairs!" Web log post. *Wordpress*. Wordpress, 04 Mar. 2009. Web. Apr.-May 2011.

Egede, Ulrik. "The Search for a Standard Model Higgs at the LHC and Electron Identification Using Transition Radiation in the ATLAS Tracker." Thesis. Lund University, 1998. *Hep.lu.se*. Lund University, 08 Jan. 1998. Web. <http://www.hep.lu.se/atlas//thesis/egede/thesis.html>.

"Finding the Higgs Boson." *The Compact Muon Solenoid Experiment European Organization for Nuclear Research*. CERN, 2008. Web. Apr.-May 2011. <http://cms.web.cern.ch/cms/Physics/HuntingHiggs/CMS.html>.

Griffiths, David. "Gauge Theories." Introduction to Elementary Particles. Weinheim: Wiley-VCH, 2008. 375-81. Print.

Grim, Kathryn. "LHC Set to Gain Major Ground in Higgs Search." Web log post. *Symmetry Breaking*. Fermilab/SLAC, 16 Mar. 2011. Web. Apr.-May 2011. <http://www.symmetrymagazine.org/breaking/2011/03/16/lhc-set-to-gain-major-ground-in-higgs-search/>.

Harvard University. Monitored Drift Tube Chambers. Tech. Cambridge: Harvard University, 1997. Print.

Horvat, Sandra. "The (long and Winding) Road to the Golden Higgs Channel." Web log post.*ATLAS E-News*. 8 Mar. 2010. Web. Apr.-May 2011. <http://atlas-service-enews.web.cern.ch/atlas-service-enews/2010/features_10/features_higgs-search.php>.

Rainwater, D. *Searching for the Higgs Boson*. Publication. Rochester: Department of Physics and Astronomy, University of Rochester, 2008. Print.

"Transition Radiation Tracker (TRT)." *The ATLAS Experiment*. CERN, 2009. Web. Apr.-May 2011. <http://atlas.ch/inner_detector3.html>.